Intramolecular Electron Transfer in *Pseudomonas aeruginosa* cd_1 Nitrite Reductase: Thermodynamics and Kinetics

Ole Farver,[§] Maurizio Brunori,[‡] Francesca Cutruzzolà,[‡] Serena Rinaldo,[‡] Scot Wherland,[¶] and Israel Pecht[†*]
[†]Department of Immunology, The Weizmann Institute of Science, Rehovot , Israel; [‡]Dipartimento di Scienze Biochimiche, Università di Roma 'La Sapienza', Roma, Italy; [§]Institute of Analytical Chemistry, University of Copenhagen, Copenhagen, Denmark; and [¶]Department of Chemistry, Washington State University, Pullman, Washington

ABSTRACT The cd_1 nitrite reductases, which catalyze the reduction of nitrite to nitric oxide, are homodimers of 60 kDa subunits, each containing one heme-*c* and one heme-d_1. Heme-*c* is the electron entry site, whereas heme-d_1 constitutes the catalytic center. The 3D structure of *Pseudomonas aeruginosa* nitrite reductase has been determined in both fully oxidized and reduced states. Intramolecular electron transfer (ET), between *c* and d_1 hemes is an essential step in the catalytic cycle. In earlier studies of the *Pseudomonas stutzeri* enzyme, we observed that a marked negative cooperativity is controlling this internal ET step. In this study we have investigated the internal ET in the wild-type and His369Ala mutant of *P. aeruginosa* nitrite reductases and have observed similar cooperativity to that of the *Pseudomonas stutzeri* enzyme. Heme-*c* was initially reduced, in an essentially diffusion-controlled bimolecular process, followed by unimolecular electron equilibration between the *c* and d_1 hemes ($k_{ET} = 4.3\ s^{-1}$ and $K = 1.4$ at 298K, pH 7.0). In the case of the mutant, the latter ET rate was faster by almost one order of magnitude. Moreover, the internal ET rate dropped (by ~30-fold) as the level of reduction increased in both the WT and the His mutant. Equilibrium standard enthalpy and entropy changes and activation parameters of this ET process were determined. We concluded that negative cooperativity is a common feature among the cd_1 nitrite reductases, and we discuss this control based on the available 3D structure of the wild-type and the H369A mutant, in the reduced and oxidized states.

INTRODUCTION

The cd_1 nitrite reductases (NiRs) (EC 1.9.3.2) constitute a family of enzymes catalyzing the single-electron reduction of nitrite to nitric oxide in bacterial energy conversion denitrification processes. Three-dimensional structures have been determined so far for *Paracoccus pantotrophus* (1) and *Pseudomonas aeruginosa* (2) NiRs. Both are homodimers of ~60 kDa subunits, each of which contains one covalently bound heme-*c* and one heme-d_1, each residing in distinct domains of the monomer. Heme-*c* is the electron entry site, whereas heme-d_1 constitutes the catalytic center where the single electron is transferred to the substrate, nitrite ion. Intramolecular electron transfer (ET), between *c* and d_1 hemes is an essential step in the catalytic cycle and has been studied by several groups (3,4). Sequence comparison of cd_1 NiRs shows a striking difference among the *P. aeruginosa*, *P. pantotrophus,* and *Pseudomonas stutzeri* (*P. stutzeri*) enzymes. We have previously investigated the internal ET in the *P. stutzeri* enzyme using the pulse radiolysis method and have measured the kinetics of ET equilibration between the *c* and d_1 heme sites (5,6) as part of a more comprehensive study of intramolecular ET in proteins initiated by pulse radiolysis (7). Significantly, the internal heme-*c* to heme-d_1 ET rate constant was found to decrease by close to three orders of magnitude upon increasing the extent of *P. stutzeri* NiR reduction from less than one electron-equivalent per mole enzyme to full reduction, resolving an allosteric control mechanism of this intramolecular process. The internal distribution of reduction equivalents between the heme sites was also shown to depend on the number of electrons taken up by the *P. stutzeri* enzyme. Static redox titrations of the cd_1 NiR enzymes isolated from both *P. aeruginosa* and *P. pantotrophus* have also demonstrated substantial cooperativity between the hemes *c* and d_1 (8,9). Reductive titrations of the *P. aeruginosa* enzyme suggested the presence of thermodynamic and probably electronic interactions between the hemes. The model used for fitting the data implied positive cooperativity between the two d_1-type hemes and negative cooperativity of similar magnitude between the two *c*-type hemes (7). However, no knowledge of the 3D structure of the *P. aeruginosa*-NiR was available at that time. Hence, the proposed model required assumptions that now need reexamination. Similarly, the 3D structure of the *P. stutzeri* enzyme has still not been determined. Hence, structural implications of our studies of this enzyme are still pending. Therefore, a detailed kinetic study by pulse radiolysis of the wild-type (WT) *P. aeruginosa*-NiR and the single-site mutant H369A (in which one of the invariant histidines on the distal side of heme-d_1 has been substituted by an alanine) has been carried out, and the results are interpreted using the available 3D structures.

MATERIAL AND METHODS

Mutagenesis and protein purification

The NiR was purified from anaerobically grown *P. aeruginosa* cells (10). Mutagenesis of His 369 to Ala, protein purification, and reconstitution with d_1 heme has been described previously (11).

Submitted June 26, 2008, and accepted for publication December 23, 2008.

*Correspondence: israel.pecht@weizmann.ac.il

Editor: Feng Gai.

0006-3495/09/04/2849/8 $2.00

doi: 10.1016/j.bpj.2008.12.3937

Kinetic measurements

Time-resolved measurements were performed on the pulse radiolysis system based on the Varian (Palo Alto, CA) V-7715 linear accelerator at the Hebrew University in Jerusalem, Israel. Five MeV accelerated electrons were employed using pulse lengths in the range 0.1–1.5 μs. To produce 1-methylnicotinamide radicals (1-MNA*), argon-saturated solutions containing 5 mM 1-MNA* and 10 mM potassium phosphate at pH 5.5–7.5 were employed. For production of CO_2^- radicals, N_2O-saturated solutions containing 100 mM sodium formate and 10 mM potassium phosphate at pH 5.5 or 7.5 were used. A 10.00 mm Spectrosil (Hellma, Müllheim, Germany) cuvette was employed, using either one or three light passes, which resulted in an overall optical path length of either 1 or 3 cm. A 150 W xenon lamp produced the analyzing light beam, together with a Bausch & Lomb (Rochester, NY) double grating monochromator. Appropriate optical filters with cutoff at 285 or 385 nm were used to reduce photochemical and light-scattering effects. For both WT and H369A *P. aeruginosa*-NiR the redox state of heme-*c* could be monitored at 551 nm, where heme-d_1 has an isosbestic point. Reduction of heme-d_1 was followed at 640 nm in the WT enzyme, whereas, in the H369A mutant, the examining wavelength was 460 nm, exploiting the different isosbestic points of heme-*c* here. The data acquisition system consisted of a Tektronix 390 A/D transient recorder (Sony-Tektronix, Tokyo, Japan) attached to a personal computer. The temperature of the reaction solutions in the cuvette (15 different temperatures in the range 2–42°C) was controlled by a thermostating system and continuously monitored by a thermistor attached to the cuvette. Reactions were generally performed under pseudo-first-order conditions, with typically a 20-fold excess of oxidized protein over reducing radicals. In each experiment, 2000 data points were collected and divided equally between two different time scales, each comprising at least three half-lives. Each kinetic run was repeated at least four times. The data were analyzed by fitting to a sum of exponentials using a nonlinear least-squares program written in MATLAB (The MathWorks, Natick, MA) to give rate constants, k_{ET}, and amplitudes. The equilibrium constants were evaluated based on the amplitude of the fast initial reduction of heme-*c* and the amplitude of the subsequent reoxidation in the following way: In each experiment the amplitude of the fast heme-*c*(III) reduction was a measure of the number of reduction equivalents added to the enzyme in this particular pulse (A_{tot}). Part of heme-*c*(II) was then being reoxidized by internal ET to heme-d_1(III). This was A_{reox}. The remaining part of the reduced heme-*c*(II) was A_{red}. Thus, for each pulse $A_{tot} = A_{reox} + A_{red}$, and $R_{551} = A_{reox}/A_{red}$. When R_{551} was plotted against the total number of reduction equivalents added to the enzyme during the pulse radiolytic reduction titration, a bell-shaped figure was obtained. A best fit was then calculated from the model using the intrinsic equilibrium constants as variables. The forward and reverse rate constants were calculated based on their relationship to the observed k_{ET} values and equilibrium constants. For example, in the initial pulses, $k_{ET} = k_{23} + k_{32}$ and $K_{23} = k_{23}/k_{32}$ (for numbering, see Scheme 1). Simulation of the observed rate constants was accomplished by implementing the mechanism displayed in Scheme 1 using the Kintecus (V. 3.2) program package, converting the species concentrations into absorbance values, and fitting absorbance versus time data, after 1 ms, to two exponentials. The simulation started with a 20 μM solution of cd_1 enzyme homodimers, then introduced a 3 μM pulse of 1-MNA* radicals. Fifty seconds were allowed for the system to evolve, and then another pulse of radicals was introduced. This was repeated for 27 pulses to produce 27 absorbance versus time data sets and to achieve full reduction.

RESULTS

The reduction of *P. aeruginosa*-NiR was investigated in several sets of experiments using either the CO_2^- or, mainly, 1-MNA* radicals, at pH 7.5, over a temperature range of 2–42°C. Almost identical results were obtained with each one of the two radicals. The reduction states of both heme types were monitored independently by measuring time-resolved absorption changes at 551 nm (for heme-*c*) and 640 nm (for heme-d_1). The initial, fast process observed at 551 nm was assigned to a bimolecular reaction proceeding at rates close to the diffusion-controlled limit where the radicals reduce heme-*c*. Interestingly, this reaction was biphasic, showing two pseudo-first-order rate constants that led to two second-order rate constants, 2.4×10^9 $M^{-1}s^{-1}$ and 4.0×10^8 $M^{-1}s^{-1}$ at 298 K (Fig. 1). Significantly, no absorption changes at 640 nm were observed in this submillisecond time range, demonstrating that the radicals do not directly reduce heme-d_1. Subsequently, a much slower decline in absorption at 551 nm and 640 nm was observed in a seconds time range. These processes were always well separated from the initial bimolecular step (Fig. 2). Because these absorption changes were found to be synchronous and concentration independent, they were assigned to an internal ET from heme-*c* to heme-d_1, analogous to the reduction pattern observed for the *P. stutzeri*-NiR. Sequential introduction of pulses into the solution resulted in an increasing degree of NiR reduction. Rate and equilibrium constants for the internal ET process were determined together (Tables 1A and 1B). The extent of enzyme reduction was calculated by adding up the observed reduction amplitudes of the initial electron uptake by heme-*c* as monitored at 551 nm. Again, analogous to the results obtained with *P. stutzeri*-NiR, increasing the enzyme's degree of reduction beyond one electron equivalent per monomer caused the internal heme-*c* to

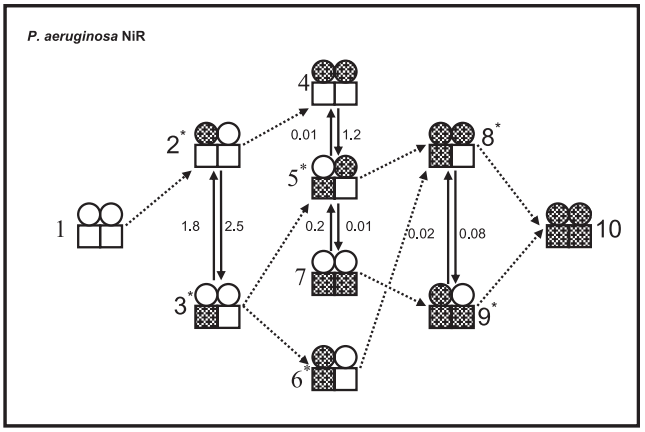

SCHEME 1 Proposed mechanism for the stepwise reduction of *P. aeruginosa*-NiR. Circles represent heme-*c* and squares heme-d_1. Open symbols represent an oxidized site; solid ones, a reduced site. Each protein subunit includes one heme-*c* and the heme-d_1. The single, dotted arrows represent the bimolecular reduction of a heme-*c* by the external reductant. These reactions are all assumed to be irreversible and to occur with the same, near diffusion controlled rate. The double, extended arrows represent reversible intramolecular electron transfer within a subunit. It is assumed that there is no intramolecular electron transfer between subunits, and that there is no intermolecular protein-protein electron transfer during the examined time domain. The asterisk indicates that there are two forms of the species. They differ by the subunit on which the electron resides. For example,  and  are the two forms of species 5. Rate constants are experimental values determined at 25°C.

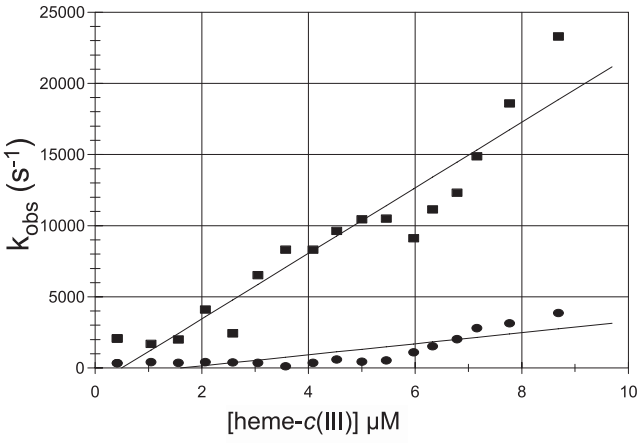

FIGURE 1 Observed rate constants of the heme-*c* fast reduction phases in WT *P. aeruginosa*-NiR plotted as function of [Fe(III)heme-*c*]. Concentrations: 9.7 μM enzyme; 5 mM 1-methyl nicotinamide; 7 mM phosphate; 0.1 M *tert*-BuOH; Anaerobic, Argon saturated. pH 7.0; optical path length 3.0 cm; pulse width 0.1 μs; temperature 25°C. Formation of Fe(II)heme-*c* was found to be bi-exponential, and the observed rate constants of the two phases are shown as ■ and •, respectively, in the plot.

heme-d_1 ET rate constant to decrease by more than one order of magnitude (e.g., from ~2 s^{-1} to <0.1 s^{-1} at 11°C), as illustrated in Fig. 3. The internal electron distribution between the *c* and d_1 hemes in each monomer was similarly found to depend on the number of reduction equivalents taken up by the enzyme (Fig. 4). The same pattern of a decline in the internal electron distribution and transfer rates has been observed over the entire temperature range examined (2–40°C). From the temperature dependence, activation parameters as well as standard enthalpy and entropy changes for the intraprotein ET are presented in Tables 1A and 1B.

The above results have been analyzed using the same model described previously (5). It assumes that electron uptake by heme-*c* is followed by equilibration between hemes *c* and d_1 within the same subunit. Intersubunit ET equilibration has been ignored, because the heme-heme separation distances in the dimer are too large (4.2 nm) (12) to allow its occurrence during the examined time domain. Similarly, intermolecular ET between enzyme dimers was not observed in the time range employed. The model depicted in Scheme 1 required only four equilibration steps where intrasubunit ET can take place.

The rate constants determined at 298 K are included in Scheme 1. The calculated, detailed internal electron distribution depends strongly on the enzyme's reduction state: In contrast to an equal partition of the first reducing equivalent between hemes *c* and d_1 observed for *P. stutzeri*-NIR, in *P. aeruginosa*-NiR, a slight preference for the latter (heme d_1) is observed ($K_{23} = 1.4$). Adding a second equivalent to *P. aeruginosa*-NiR favors species 5 ($K_{45} = 120$ and $K_{75} = 20$); i.e., the enzyme molecules that prevail have one heme site (*c* or d_1) in distinct subunits reduced. As far as the distribution of the third equivalent is concerned, preference is found for species 9, namely having both hemes d_1 reduced ($K_{89} = 4.0$). The marked decrease in observed internal ET rate constant with the extent of reduction of the enzyme is similar to that measured for *P. stutzeri*, although somewhat less extreme; a factor of 40 is measured in *P. aeruginosa*-NiR, whereas the factor is 200 in *P. stutzeri*, both at 25°C. The observed intramolecular rate constant reflects the ET process of the predominant species present at each pulse.

We have also studied the reduction pattern and internal ET rates in the single-site H369A mutant of the *P. aeruginosa* enzyme (cf. Figs. 2 and 3). It is noteworthy that the observed internal ET rates were significantly faster: at 25°C, a rate constant of 24.5 s^{-1} was determined—i.e., almost one order of magnitude larger than that measured for the WT enzyme (cf. Tables 1A and 1B). Similarly, a decrease in the internal ET rates upon increased reduction was also seen in the mutant with the rate constant leveling off at 0.8 s^{-1}.

DISCUSSION

We have investigated the reduction process of *P. aeruginosa*-NiR using the pulse radiolysis method by employing 1-MNA* and CO_2^- radicals as reductants. These pulse radiolytically produced radicals were found to directly reduce only the heme-*c*, as in *P. stutzeri*-NiR (6) as well as in earlier pulse radiolysis studies of the *P. pantotroph*us and *P. aeruginosa*-NiRs (Table 2); however, the current observation of two distinct phases of heme-*c* reduction is a feature not observed in the previous pulse-radiolysis studies of any NiR. Still, in studies of *P. aeruginosa*-NiR reduction by excess reduced azurin or chromium(II) ions, two concentration-dependent phases were also observed. This was explained by hypothesizing the existence of two different enzyme populations (14). In that study (14), the reducing agent was in large excess, whereas, in the presented study, the protein sites in excess; nevertheless, heterogeneity of the heme-*c* reduction rate was still observed. The currently observed two reduction phases cannot represent reduction of two distinct enzyme populations (e.g., two forms of the heme-*c* in the dimer), because this situation would lead to a pseudo-first-order process in which the observed rate constant would be the sum of the two individual rate constants. Instead, we suggest that the two phases could be the result of two consecutive processes in which heme-*c* Fe(III) first undergoes reduction, followed by a structural rearrangement causing spectral changes at 551 nm.

The subsequent, slower reaction observed in *P. aeruginosa*-NiR solutions involved the synchronous oxidation of heme-*c* and reduction of heme-d_1, both independent of protein concentration, and the reaction is therefore attributed to the internal (heme-*c* to heme-d_1) electron transfer process.

Both our earlier study and this pulse radiolysis study of NiRs isolated from *P. stutzeri* (5) and *P. aeruginosa,* respectively, took advantage of the possibility of gradual reduction

of the enzymes by sequential pulses and resolved the marked dependence of the internal ET rate on the degree of the reduction. This procedure apparently was not feasible in other pulse radiolysis studies of NiRs (4,13). Early kinetic studies by pulse radiolysis of cd_1 NiRs isolated from *P. aeruginosa* (13), *P. pantotrophus* (4), and *P. stutzeri* (5) yielded considerably different rate constants for this step: ~3 s^{-1}, 1400 s^{-1}, and 23 s^{-1}, respectively, at 298 K and pH 7.0 (Table 2). The rate constant for heme-*c* to heme-d_1 ET measured for the fully oxidized NiR in this study (k_{ET} = 4.3 s^{-1}) is in agreement with the rate measured by Kobayashi et al. (13) and is of the same order of magnitude as is the turnover number of *P. aeruginosa*-NiR at pH 7.0°C and 20°C (4–6 sec^{-1}) (15). Previous kinetic studies carried out by stopped-flow on the *P. aeruginosa* enzyme yielded somewhat slower rates for the heme-*c* to heme-d_1 ET (14,16,17)

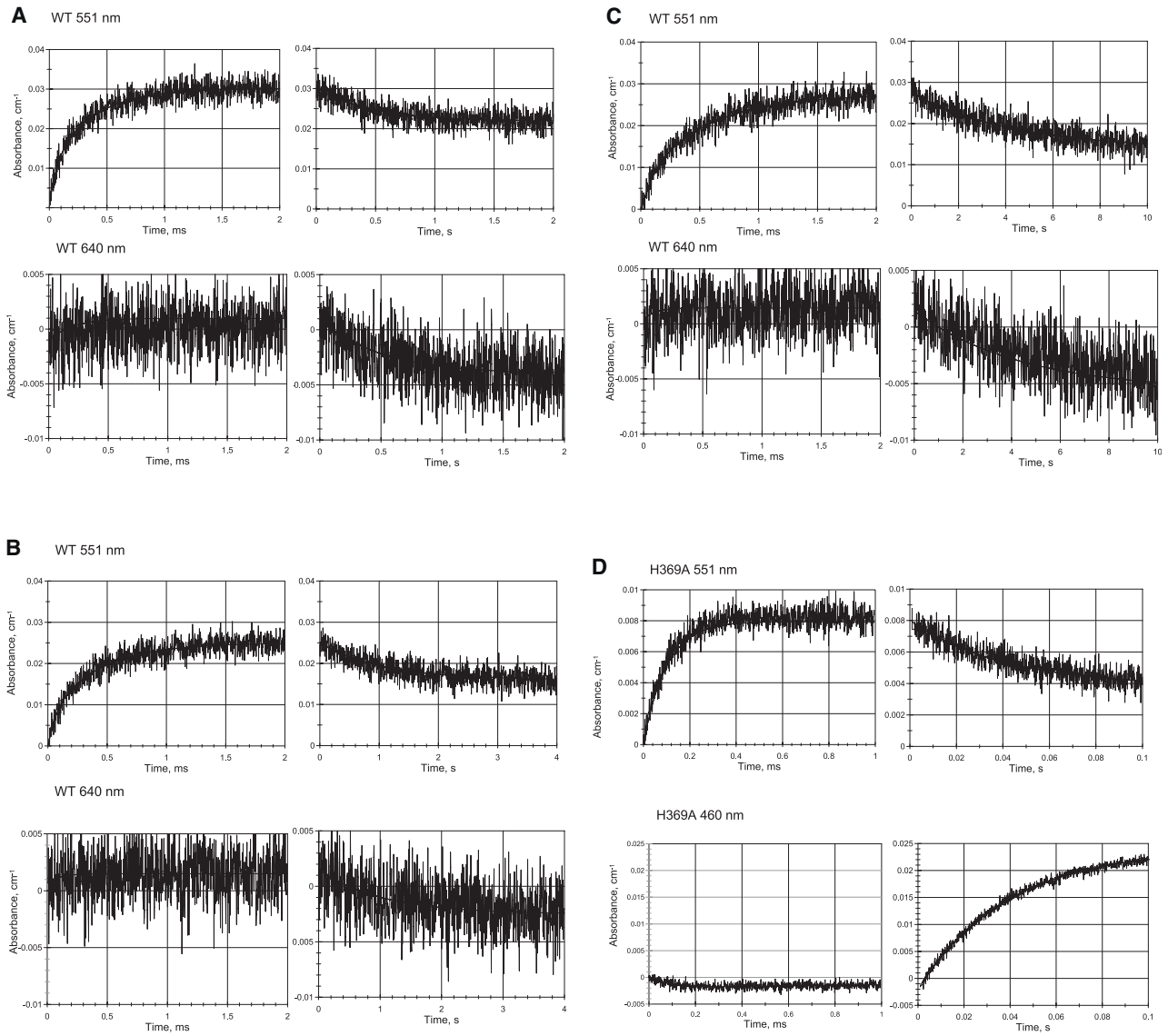

FIGURE 2 Time-resolved absorption changes upon reduction by 1-MNA* radicals. Concentrations: WT *P. aeruginosa*-NiR 9.6 μM, 5 mM 1-methyl nicotinamide, 5 mM phosphate, 0.1 M *tert*-BuOH, argon saturated, pH 7.0. Optical path length 3.0 cm, pulse width 0.1 μs, temperature 11.2°C. Measurements were performed at 551 nm, monitoring heme-*c* reduction (*left panel: fast time scale*) and heme-*c* reoxidation (*right panel: slow time scale*), and at 640 nm, monitoring heme-d_1 reduction (*left panel: fast time scale*) and heme-d_1 reoxidation (*right panel: slow time scale*). (*A*) WT initial pulses after <0.5 reduction equivalents were added. (*B*) WT after addition of ~1.1 reduction equivalents were added. (*C*) WT after addition of ~2.1 reduction equivalents were added. Concentrations: H369A *P. aeruginosa*-NiR mutant 48 μM, 2 mM 1-methyl nicotinamide, 10 mM phosphate, 0.1 M *tert*-BuOH, argon saturated. pH 7.0 Optical path length 3.0 cm, pulse width 1.0 μs; temperature 25.0°C. Measurements were performed at 551 nm, monitoring heme-*c* reduction (*left panel: fast time scale*) and heme-*c* reoxidation (*right panel: slow time scale*) and at 460 nm, monitoring heme-d_1 reduction (*left panel: fast time scale*) and heme-d_1 reoxidation (*right panel: slow time scale*). (*D*) H369A. Initial pulses after <0.5 reduction equivalents were added. (*E*) H369A, after addition of ~1.1 reduction equivalents were added. (*F*) H369A, after addition of ~2.1 reduction equivalents were added. Note that, in the case of the mutant, the rate of the faster phase at 551 nm is greater than that with the WT, consistent with the higher enzyme concentration employed.

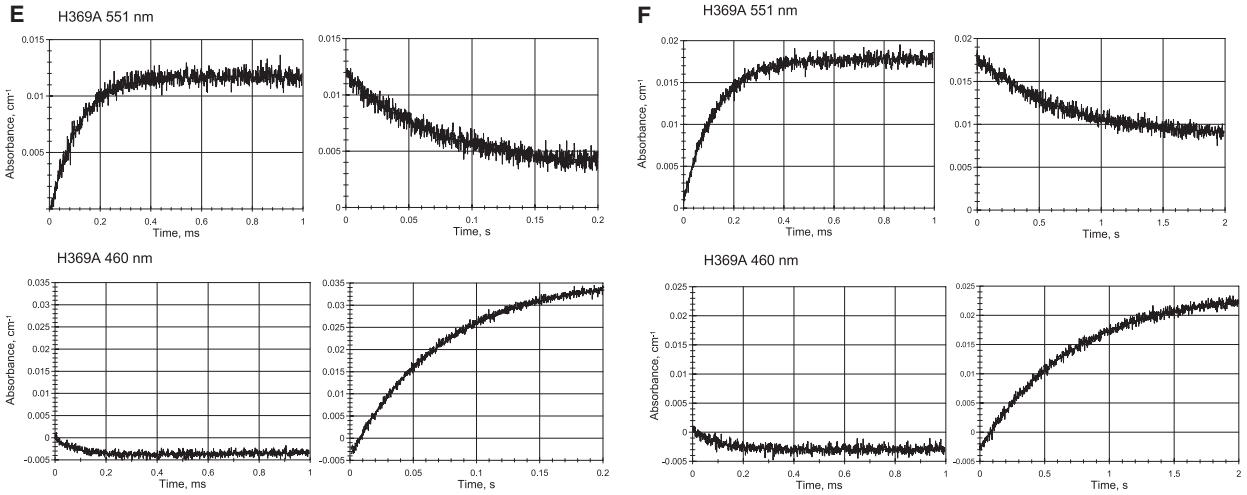

FIGURE 2 (Continued)

(Table 2), probably reflecting the different experimental conditions employed (e.g., rates obtained in this study at high degrees of NiR reduction). Because internal ET to heme-d_1 is required for nitrite reduction, only steps 2→3 and 4→5 in Scheme 1 are candidates for participating in the catalytic cycle. However, the presence of nitrite and its preferential binding to heme-d_1 are expected to change the reduction potential of this site and possibly the rates of formation of species 3 and beyond. Nitric oxide (NO) is the final product of nitrite reduction at the reduced heme-d_1 site. The stability constant for heme-d_1 Fe(II) complex formation with NO is in the range 10^7-10^8 M^{-1}, markedly different from that of most reduced heme proteins, which display higher affinities, usually ~10^{11} M^{-1}. The lower affinity of reduced *P. aeruginosa*-NiR is mainly due to an unexpectedly high rate of dissociation ($k_{off} = 70$ s^{-1}) (15), excluding significant product inhibition by NO binding to reduced heme-d_1. If NO also binds to the oxidized heme-d_1, then the reduction potential of this site, as well as the heme-*c* to heme-d_1 electron transfer rate constant, would be enhanced. It has indeed been observed in our earlier experiments (S. Wherland and I. Pecht, unpublished results) that adding NO to partially reduced *P. stutzeri*-NiR caused reoxidation of the heme-*c*, presumably by inducing intramolecular electron transfer to the oxidized heme-d_1-NO complex.

TABLE 1A Kinetics and thermodynamics of heme-*c* to heme-d_1 intramolecular ET process in WT *P. aeruginosa*-NiR at 298 K

Kinetic parameters	k/s^{-1}	$\Delta H^{\ddagger}$/kJ mol^{-1}	$\Delta S^{\ddagger}$/J K^{-1} mol^{-1}
forward, k_{23}	2.5 ± 0.3	84.8 ± 7.2	+47 ± 4
reverse, k_{32}	1.8 ± 0.2	44.5 ± 8.5	−91 ± 17
Equilibrium parameters	K_{23}	ΔH^0/kJ mol^{-1}	ΔS^0/J K^{-1} mol^{-1}
	1.4 ± 0.1	40.4 ± 4.7	+139 ± 16

Data are presented for the initial, first electron equilibration.

For WT *P. aeruginosa*-NiR, the rate-limiting step of the catalytic cycle in the presence of nitrite could be the rate of the first and second reduction equivalents arriving at the ligand-free heme-d_1 to form species 3 and 5. These species then bind nitrite, and the steps afterward (ET, protonation, water, and NO dissociation) could be fast, in agreement with recent results obtained for the *P. pantotrophus*-NiR, showing that pseudoazurin may act as an electron mediator between enzyme molecules having different reduction states, thereby accelerating the observed catalytic rate of nitrite reduction (18). Therefore, the rate of formation of species 3 and 5, which should be unaffected by nitrite, controls the overall catalytic reaction rate in WT *P. aeruginosa*-NiR.

We have also examined the internal ET in the single-site mutant of the *P. aeruginosa*-NiR, where the invariant His369 on the distal side of heme-d_1 has been substituted with Ala and is catalytically inactive toward nitrite (11). The internal ET rate was found to be significantly faster ($k_{ET} = 24.5$ s^{-1} at 298 K) when <1 electron equivalent has been added, almost one order of magnitude larger than that observed for the WT enzyme.

First we wish to present a possible structural interpretation for the different internal ET rates observed for the NiR species. Examination of available structural data obtained

TABLE 1B Kinetics and thermodynamics of heme-*c* to heme-d_1 intramolecular ET process in H369A *P. aeruginosa*-NiR at 298 K

Kinetic parameters	k/s^{-1}	$\Delta H^{\ddagger}$/kJ mol^{-1}	$\Delta S^{\ddagger}$/J K^{-1} mol^{-1}
forward, k_{23}	12.8 ± 1.6	53 ± 10	−48 ± 8
reverse, k_{32}	11.7 ± 1.5	58 ± 10	−32 ± 5
Equilibrium parameters	K_{23}	ΔH^0/kJ mol^{-1}	ΔS^0/J K^{-1} mol^{-1}
	~1.1	Not determined	Not determined

Data are presented for the initial, first electron equilibration.
Because of the limited amount of the H369A mutant, the results are based on measurements at three different temperatures, only.

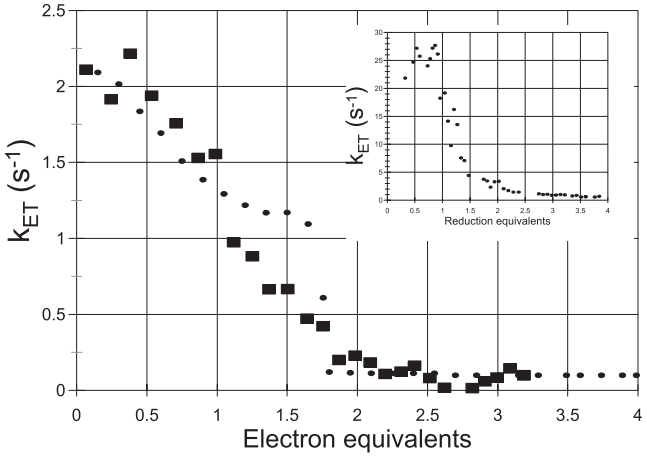

FIGURE 3 (*A*) The observed (■) and simulated (•) rate constants of intramolecular ET in *P. aeruginosa*-NiR at 11.2°C as a function of the state of reduction of the enzyme based on 551 nm absorption (reoxidation of reduced heme-*c*). The simulation represents the dominant process obtained by simulating the mechanism in Scheme 1 as described above for 27 pulses of 1-MNA* radicals, resulting in complete reduction of the four sites. The rate constants (s^{-1}) used for this temperature were: k_{23}, 0.60; k_{32}, 1.5; k_{45}, 0.35; k_{54}, 0.0046; k_{57}, 0.0010; k_{75}, 0.049; k_{89}, 0.082; and k_{98}, 0.018. (*B*) Observed rate constants of intramolecular heme-*c* to heme-d_1 ET in the H369A mutant of *P. aeruginosa*-NiR based on 551 and 460 nm data, plotted as a function of the reduction state of the enzyme at 25°C.

by crystallography of WT *P. aeruginosa*-NiR (2) suggests that dissociation of the OH^- bound on the distal side of the heme-d_1 Fe(III) may be involved in rate control. The possible importance of the Fe(III) heme-d_1 ligand OH^- in controlling the internal ET rate was suggested by Kobayashi et al. (13), based on pulse radiolysis experiments on *P. aeruginosa*-NiR. The structure of the oxidized form shows the OH^- to be stabilized by interactions with Tyr-10, protruding into the active site and originating from the partner monomer

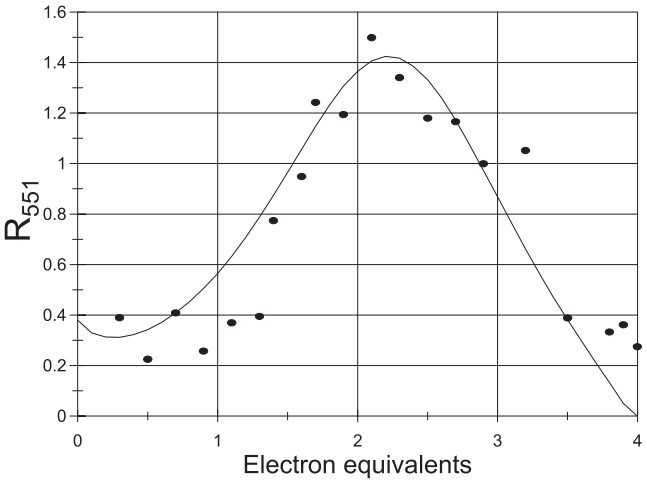

FIGURE 4 R_{551} is the ratio between reduced and reoxidized heme-*c* produced in each pulse radiolysis experiment. The curve represents the best fit to the experimental data at 11.2°C based on the reaction mechanism presented in Scheme 1.

TABLE 2 Rate constants for intramolecular ET in nitrite reductases from different sources

Source	k_{ET}/s^{-1}	Conditions	Reference
Pseudomonas aeruginosa	4.3*	pH 7.0; 298 K	The presented study
Pseudomonas aeruginosa H369A mutant	24.5*	pH 7.0; 298 K	The presented study
Pseudomonas aeruginosa	3.0*	pH 7.0; 298 K	13
Pseudomonas aeruginosa	0.25–0.81†	pH 7.0; 298 K	14,16,17
Paracoccus pantotrophus	1400*	pH 7.0	4
Pseudomonas stutzeri	23*	pH 7.0; 298 K	5

*Measured by pulse radiolysis.
†Measured by stopped flow.

(2). This is a remarkable case of ''domain swapping'', which is typical of *P. aeruginosa*-NiR (2) activity, but not observed in the oxidized *P. pantotrophus*-NiR (1). Moreover, it should be added that, upon reduction, Tyr-10 changes its conformation (19), and this slippage is associated with disappearance of the hydroxide ion from the active site pocket. It was also shown (11,20) that binding of anions to heme-d_1 is stabilized by the two invariant distal His; therefore, it may be anticipated that stability of the Fe(III)-bound OH^- would decrease if one or both His were removed. The observation that the heme-*c* to heme-d_1 internal ET rate constant is increased by ~10-fold in the His369A mutant seems consistent with this hypothesis.

The second and more intriguing observation is the decrease in the internal heme-*c* to heme-d_1 ET rate constant (by more than one order of magnitude) as the number of electrons pumped in is increased, as shown in Fig. 3 for the WT enzyme. Modeling of the current results requires the assumption of site-site interaction within a dimer. After one reducing equivalent has been taken up by the enzyme, the rate constant declines to a value approximately one half of the maximum value of 2 s^{-1} (at 11°C in Fig. 3). However, a more dramatic drop in rate constant is observed upon addition of more reducing equivalents, as the second heme-d_1 starts being reduced. In both the WT and the H369A mutant the heme-*c* to heme-d_1 rate constant drops as the fractional reduction increases, by approximately the same amount (~30-fold), leveling off at 0.08 s^{-1} at 25°C in WT. These results provide clear kinetic evidence for negative cooperativity between the two heme-d_1 sites in the dimer. Using the 3D structures now available for oxidized and reduced *P. aeruginosa*-NiR (2,19), we present below a structural hypothesis for this remarkable effect.

The rate constants observed for the individual internal ET steps (Scheme 1) deserve attention in the context of the 3D structure. Using the separation distance between the iron centers of the two hemes in one monomer, 2.0 nm (2,19), we calculate the expected species 2 → species 3 intramolecular ET rate constant in the activationless case to be $k_{MAX} \approx 10^4\ s^{-1}$. The experimentally observed rate constant is 2.5 s^{-1} and the driving force, $-\Delta G^0$, is 0.009 eV ($K = 1.4$ at 298 K). From these we may calculate a reorganization

energy for heme-*c* to heme-d_1 ET of 0.87 eV (84 kJ/mol^{-1}). This is typical for *c*-type heme reorganization, 0.8 eV (21). The 30-fold drop in rate constant to 0.08 s^{-1} mentioned in the previous paragraph precludes changes in the driving force having a major influence, because this would require a $K_{89} = 0.002$ for the heme-*c* to heme-d_1 electron equilibration, whereas the observed equilibrium constant is 4.0 (Scheme 1). Changes in reorganization energy alone would require an increase of no less than 0.35 eV, which appears quite unrealistic. Hence, this observed decrease in rate must involve changes taking place in the 3D structure of the enzyme. Several conformational differences between reduced and oxidized *P. aeruginosa*-NiR have been reported (13), which may provide a rationale for the steep decline in rates shown in Fig. 3. Structural changes causing a decrease in the electronic coupling between donor and acceptor may in principle lead to a decrease in ET rate constant (21). Thus, for instance, breaking one hydrogen bond, forcing a through-space jump, could account for a ~50-fold drop in rate constant. Candidates for such hydrogen bonds in the *P. aeruginosa*-NiR structure have been identified as two water molecules bridging hemes *c* and d_1 (2). An important redox-linked conformational change was observed by crystallography: In the reduced form, a loop (residues 56–62) belonging to the heme-*c* domain moves to form a hydrogen bond between Thr-59 and Gln-11 (coming from the N-terminal arm), as shown in Fig. 5.

In summary, we propose that the observed allosteric control of the rate constants for intramolecular electron transfer between the hemes is a result of a complex interplay among several conformational changes occurring upon reduction and resolved by the 3D structural analysis—namely, the relocation of Tyr-10, the coupled dissociation of the OH^- ligand, and the disruption of the hydrogen bonds at the interface between the two heme domains (see Fig. 5). This interpretation is consistent with the finding that intramolecular ET is faster in the H369A mutant, given the decrease of positive charge density on the distal side of heme-d_1.

The mechanism of communication between monomers, underlying the decrease in ET rate with the extent of the enzyme's reduction (Fig. 3), is not immediately apparent but may be interpreted as follows: The structural analysis resolved a rather large sliding motion of the whole heme-*c* domain relative to the heme-d_1 domain in the His mutants (11,12). This rather large conformational change was not observed upon reduction of the WT enzyme (19); however, we assume that this is due to the fact that the structure of the reduced WT was obtained by reduction of oxidized crystals rather than by crystallization of the reduced protein, possibly imposing a constraint that prevented this transition. In fact, in the case of *P. pantotrophus*-NiR, Hajdu and coworkers (23) observed a large heme-*c* domain rotation only when the enzyme was crystallized in the reduced state. Therefore, we propose that allosteric communication between identical monomers may depend on a perturbation of the domain-domain interface within each monomer and a coupled large relocation of the heme-*c* domain, upon reduction of the enzyme. These conformational changes perturb the above-mentioned hydrogen bonds, decreasing the electronic coupling between heme-*c* and heme-d_1. Thus, control of the electron transfer rates involves contributions from local changes, affecting the driving force of the intramolecular ET, and more global changes (such as the relocation of the

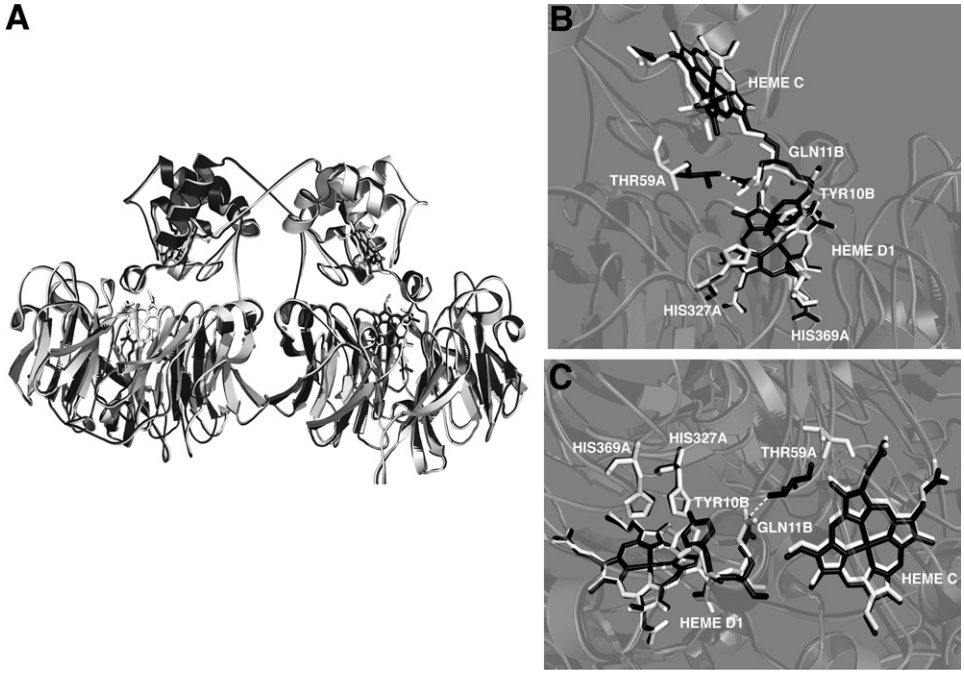

FIGURE 5 Conformational changes occurring upon reduction of *P. aeruginosa*-NiR. (*A*) Superposition of the 3D structure of the oxidized (*white*) and reduced (*black*) dimeric enzyme, highligthing the swapping of the N-termini. Two different views (*B* and *C*) of the interface between the heme-*c* and heme-d_1 domains in the two oxidation states are presented. Three relevant residues in the heme-d_1 pocket are depicted: His-369 and His-327 belonging to monomer A (*HIS-327A* and *HIS-369A*), and Tyr-10 coming from the other monomer B (*TYR-10B*). The reorganization of the 56-62 loop and the new H-bond (*dashed line*) between Thr-59 (from monomer A) and Gln-11 (from monomer B) formed upon reduction are shown (*THR-59A* and *GLN-11B*).

c-heme versus d_1-heme domains), which may affect the electronic coupling between sites (within and between monomers), further increasing the energy barrier for ET as the enzyme undergoes reduction.

O.F. acknowledges the generous support extended by the Kimmelman Center for Biomolecular Structure and Assembly at the Weizmann Institute of Science. We thank Mr. Eran Gilad of the Hebrew University in Jerusalem for his excellent technical support in running the accelerator.

These studies were supported by grants from Ministero della Università e Ricerca of Italy (RBIN04PWNC_000 to M.B. and RBIN04PWNC_002 to F.C.) and from the Ministero degli Affari Esteri of Italy (L.401/90-2006) to M.B. for supporting the Italy-Israel research project.

REFERENCES

1. Fülöp, V., J. W. B. Moir, S. J. Ferguson, and J. Hajdu. 1995. The anatomy of a bifunctional enzyme: structural basis for reduction of oxygen to water and synthesis of nitric oxide by cytochrome cd_1. *Cell.* 81:369–377.
2. Nurizzo, D., M.-C. Silvestrini, M. Mathieu, F. Cutruzzolà, D. Bourgeois, et al. 1997. N-terminal arm exchange is observed in the 2.15 Å crystal structure of oxidized nitrite reductase from *Pseudomonas aeruginosa*. *Structure.* 5:1157–1171.
3. Silvestrini, M. C., M. G. Tordi, G. Musci, and M. Brunori. 1990. The reaction of *Pseudomonas* nitrite reductase and nitrite. A stopped-flow and EPR study. *J. Biol. Chem.* 265:11783–11787.
4. Kobayashi, K., A. Koppenhoefer, S. J. Ferguson, and S. Tagawa. 1997. Pulse radiolysis studies on cytochrome cd_1 nitrite reductase from *Thiosphaera pantotropha*: evidence for a fast intramolecular electron transfer from c-heme to d_1-heme. *Biochemistry.* 36:13611–13616.
5. Farver, O., P. M. H. Kroneck, W. G. Zumft, and I. Pecht. 2002. Intramolecular electron transfer in cytochrome cd_1 nitrite reductase from *Pseudomonas stutzeri*; kinetics and thermodynamics. *Biophys. Chem.* 98:27–34.
6. Farver, O., P. M. H. Kroneck, W. G. Zumft, and I. Pecht. 2003. Allosteric control of internal electron transfer in cytochrome cd_1 nitrite reductase. *Proc. Natl. Acad. Sci. USA.* 100:7622–7625.
7. Farver, O., and I. Pecht. 2007. Elucidation of electron-transfer pathways in copper and iron proteins by pulse radiolysis experiments. *Prog. Inorg. Chem.* 55:1–78.
8. Blatt, Y., and I. Pecht. 1979. Allosteric cooperative interactions among redox sites of *Pseudomonas* cytochrome oxidase. *Biochemistry.* 18:2917–2922.
9. Koppenhofer, A., K. L. Turner, J. W. A. Allen, S. K. Chapman, and S. J. Ferguson. 2000. Cytochrome cd_1 from *Parococcus pantotrophus* exhibits kinetically gated, conformationally dependent, highly cooperative two-electron redox behavior. *Biochemistry.* 39:4243–4249.
10. Parr, S. R., D. Barber, and C. A. Greenwood. 1976. A purification procedure for the soluble cytochrome oxidase and some other respiratory proteins from *Pseudomonas aeruginosa*. *Biochem. J.* 157:423–430.
11. Cutruzzolà, F., K. Brown, E. K. Wilson, A. Bellelli, M. Arese, et al. 2001. The nitrite reductase from *Pseudomonas aeruginosa*: essential role of two active-site histidines in the catalytic and structural properties. *Proc. Natl. Acad. Sci. USA.* 98:2232–2237.
12. Brown, K., V. Roig-Zamboni, F. Cutruzzolà, M. Arese, W. L. Sun, et al. 2001. Domain swing upon His to Ala mutation in nitrite reductase of *Pseudomonas aeruginosa*. *J. Mol. Biol.* 312:541–554.
13. Kobayashi, K., A. Koppenhoefer, S. J. Ferguson, N. J. Watmough, and S. Tagawa. 2001. Intramolecular electron transfer from c heme to d_1 heme in bacterial cytochrome cd_1 nitrite reductase occurs over the same distances at very different rates depending on the source of the enzyme. *Biochemistry.* 40:8542–8547.
14. Parr, S. R., D. Barber, C. Greenwood, and M. Brunori. 1977. The electron-transfer reaction between azurin and the cytochrome c oxidase from *Pseudomonas aeruginosa*. *Biochem. J.* 167:447–455.
15. Rinaldo, S., A. Arcovito, M. Brunori, and F. Cutruzzolà. 2007. Fast dissociation of nitric oxide from ferrous *Pseudomonas aeruginosa* cd_1 nitrite reductase: a novel outlook on the catalytic mechanism. *J. Biol. Chem.* 282:14761–14767.
16. Schichman, S. A., and H. B. Gray. 1981. Kinetics of the anaerobic reduction of ferricytochrome-cd_1 by $Fe(EDTA)^2$—evidence for bimolecular and intramolecular electron transfers to the d_1 hemes. *J. Am. Chem. Soc.* 103:7794–7795.
17. Cutruzzolà, F., M. Arese, S. Grasso, A. Bellelli, and M. Brunori. 1997. Mutagenesis of nitrite reductase from *Pseudomonas aeruginosa*: tyrosine-10 in the c heme domain is not involved in catalysis. *FEBS Lett.* 412:365–369.
18. Sam, K. A., S. A. Fairhurst, R. N. F. Thorneley, J. W. A. Allen, and S. J. Ferguson. 2008. Pseudoazurin dramatically enhances the reaction profile of nitrite reduction by *Paracoccus pantotrophus* cytochrome cd_1 and facilitates release of product nitric oxide. *J. Biol. Chem.* 283:12555–12563.
19. Nurizzo, D., F. Cutruzzolà, M. Arese, D. Bourgeois, M. Brunori, et al. 1998. Conformational changes occurring upon reduction and NO binding in nitrite reductase from *Pseudomonas aeruginosa*. *Biochemistry.* 37:13987–13996.
20. Sun, W., M. Arese, M. Brunori, D. Nurizzo, K. Brown, et al. 2002. Cyanide binding to cd1 nitrite reductase from *Pseudomonas aeruginosa*: role of the active-site His369 in ligand stabilization. *Biochem. Biophys. Res. Commun.* 291:1–7.
21. Gray, H. B., and J. R. Winkler. 2003. Electron tunneling through proteins. *Q. Rev. Biophys.* 36:341–372.
22. Beratan, D. N., J. N. Betts, and J. N. Onuchic. 1991. Protein electron-transfer rates set by the bridging secondary and tertiary structure. *Science.* 252:1285–1288.
23. Sjögren, T., and J. Hajdu. 2001. The structure of an alternative form of *Paracoccus pantotrophus* cytochrome cd_1 nitrite reductase. *J. Biol. Chem.* 276:29450–29455.